Threshold-based Wireless-based NOMA Systems over Log-Normal Channels: Ergodic Outage Probability of Joint Time Allocation and Power Splitting Schemes

Hoang Thien Van[1], Quyet-Nguyen Van[2], Danh Hong Le[3, *], Lukas Sevcik[4, 5], Nguyen Hoang Duy[1], Hoang-Sy Nguyen[6], Miroslav Voznak[7]
[1]The Saigon International University, Ho Chi Minh City, Vietnam
[2]Faculty of Technology, Dong Nai Technology University, Bien Hoa City, Dong Nai Province, Vietnam
[3]Van Hien University, Ho Chi Minh City, Vietnam
[4]Faculty of Electrical Engineering and Information Technology, University of Zilina, 01026 Zilina, Slovakia
[5]Research Centre University of Zilina, 01026 Zilina, Slovakia
[6]Binh Duong University, Thu Dau Mot City, Binh Duong Province, Vietnam
[7]VSB - Technical University of Ostrava, 17. listopadu 15/2172, 708 33 Ostrava-Poruba, Czech Republic
danhlh@vhu.edu.vn

***Abstract*—Due to the development of state-of-the-art fifth-generation communication (5G) and Internet-of-Things (IoT), the demands for capacity and throughput of wireless networks have increased significantly. As a promising solution for this, a radio access technique, namely, non-orthogonal multiple access (NOMA) has been investigated. Particularly, in this paper, we analyse the system performance of a joint time allocation and power splitting (JTAPS) protocol for NOMA-based energy harvesting (EH) wireless networks over indoor scenarios, which we modelled with log-normal fading channels. Accordingly, for the performance analysis of such networks, the analytical expression of a metric so-called "ergodic outage probability" was derived. Then, thanks to Monte Carlo simulations done in Matlab, we are able to see how different EH power splitting (PS) and EH time switching (TS) factors influence the ergodic outage probability. Last, but not least, we plot the simulation results along with the theoretical results for comparison studies.**

Manuscript received 14 October, 2020; accepted 28 April, 2021.

This work was partially supported by Slovak Research and Development Agency under Grant No. APVV-16-0505 (Project title: "The short-term prediction of photovoltaic energy production for needs of power supply of intelligent buildings - PREDICON", by Slovak VEGA Grant Agency under Grant No. 1/0626/19 (Project title: "Research of mobile objects localization in IoT environment"), and by the project of Operational Programme Integrated Infrastructure: Independent research and development of technological kits based on wearable electronics products as tools for raising hygienic standards in a society exposed to the virus causing the COVID-19 disease (ITMS code 313011ASK8). The project is co-funded by European Regional Development Fund. Finally, thanks for the Saigon International University (SIU) funds for supporting this project.

***Index Terms*—Non-orthogonal multiple access; Energy harvesting; Log-normal fading; Joint time allocation and power splitting; Ergodic outage probability.**

I. INTRODUCTION

The non-orthogonal multiple access (NOMA) has attracted a vast amount of research owing to the fact that it can support massive connectivity with low latency, high fairness, high reliability, and high throughput [1]–[4]. In general, there are power and code-domain NOMA. For our study, we can employ the power domain, which can superimpose multiple devices in one power domain, then multiplex them to exploit the channel gain difference [5]. Besides, we can gain benefit from the deployment of multiple devices by using simultaneous wireless information and power transfer (SWIPT) technology. Indeed, the combination NOMA and SWIPT have been investigated widely in [6]–[11]. According to the works in [6]–[9], the systems with NOMA and SWIPT significantly outperform the conventional orthogonal multiple access (OMA) systems. The data rates in such systems depend on the transmission resource allocation in the uplink (UL) and the downlink (DL) [10]. Paper [11] employed the massive access in the NOMA IoT networks and optimized systems.

Furthermore, there are a number of studies related to the SWIPT cooperative relaying networks [12]–[19] that employ either TS, PS relaying protocols or a hybrid version of the two to improve the system performance. From the

studies, it can be drawn that the hybrid version performs notably better than the two standalone relaying protocols. As a step further, the application of NOMA on SWIPT cooperative relaying networks was considered by the authors in [19]–[23]. In such networks, device users are utilized as relays, which help the information transmission between the source and other distant device users. Being SWIPT-based, the device users can harvest energy from the source signal to power themselves, subsequently providing higher throughput and energy efficiency gains in comparison with conventional relaying systems. These self-sustaining systems, indeed, are highly applicable for IoT devices, e.g., in solar panels for power output measuring purposes [24], or in the applications of emerging intelligent textiles [25]–[27].

It should be noted that for most of the cooperative wireless network studies, the fading channels are specified by popular outdoor fading models, such as Nakagami-m, Rayleigh, etc. In fact, little attention has been paid on indoor fading models, such as log-normal. In particular, log-normal fading is excellent for modelling indoor fading effects owing to building walls, in-house obstacles, and human movements [28]–[30], making it more appropriate for IoT applications. However, the number of studies, which applied log-normal fading channels in cooperative relaying networks, is limited [31]–[35].

Inspired by the above studies, we investigate in this paper the ergodic outage probability of the joint time allocation and power splitting (JTAPS) scheme in NOMA-based SWIPT networks. Following the introduction, Section II is dedicated to the system model. In Section III, we derive the ergodic outage probability of each user in the JTAPS protocol for the considered network over log-normal fading channels. Section IV presents the results from the simulation. This paper is concluded in Section V.

II. System Model

Figure 1 illustrates the system model with a base station (BS), one user near to S (UN), and another far from S (UF). To avoid the obstacle between S and UF, we have data sent from BS to UN, then forwarded to UF. Thereby, we operate UN with DF mode and sustain it with the energy harvested from BS. Additionally, we denote the BS – UN and UN – UF distances, consecutively, as d_A and d_B, with complex channel coefficients of h_A and h_B. Besides, we consider two independently and identically distributed (i.i.d.) random variables (RVs) over the block time following log-normal model, being $|h_A|^2$ and $|h_B|^2$. They are respectively specified with parameters $LN\left(\mu_{h_A}, \sigma^2_{h_A}\right)$ and $LN\left(\mu_{h_B}, \sigma^2_{h_B}\right)$. Last, but not least, we have the mean value of $10\log\left(\mu_{h_i}\right)$ and the standard deviation of $10\log\left(\left|\sigma_{h_i}\right|^2\right)$, $i \in \{A, B\}$, denoted as μ_{h_i} and $\sigma^2_{h_i}$, respectively.

As shown in Fig. 2, for the hybrid JTAPS scheme, the transmission time T is split into three blocks, one αT and two $(1-\alpha)T/2$, with time switching factor $\alpha \in [0,1]$ [13]. The first $(1-\alpha)T/2$ block, within which UN receives signal power P_S from BS, is further split into βP_S and $(1-\beta)P_S$, respectively, for energy harvesting (EH) and data transmission from BS to UN with the power splitting factor $\beta \in [0,1]$. Within the second $(1-\alpha)T/2$ block, we use all harvested energy for data transmission from UN to UF.

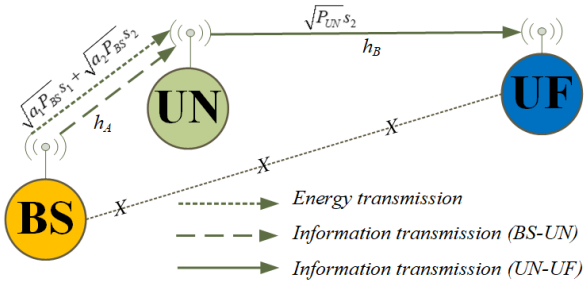

Fig. 1. System Model.

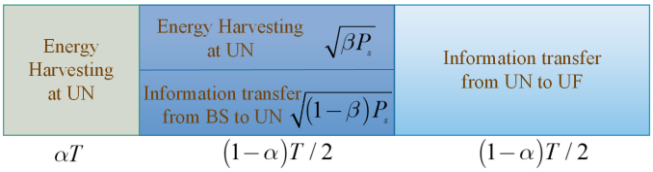

Fig. 2. JTAPS scheme.

III. Performance Analysis

A. From BS to UN: Energy Harvesting and Information Transmission

Within the first EH block, αT, we can harvest energy with an amount of

$$E_{H1} = \eta T \frac{\alpha P_S |h_A|^2}{d_A^m}, \tag{1}$$

where $0 < \eta < 1$ stands for the EH efficiency at UN, specified by the rectifier and EH circuitry that we employ at UN.

Similarly, during the first $(1-\alpha)T/2$, the harvested energy at UN is

$$E_{H2} = \eta \beta T \frac{(1-\alpha) P_S |h_A|^2}{2 d_A^m}. \tag{2}$$

Subsequently, the UN transmit power during the second $(1-\alpha)T/2$ is

$$P_{UN} = \frac{E_{H1} + E_{H2}}{(1-\alpha)T/2} = \frac{\eta[2\alpha + (1-\alpha)\beta] P_S h_A^2}{(1-\alpha) d_A^m}. \tag{3}$$

It should be noted that from a power allocating perspective, we should assign more power to UF because it is located further from BS than UN. Thereby, we allocate the power allocation coefficients a_1 and a_2, ($a_2 > a_1 > 0$ and $a_1 + a_2 = 1$), respectively, for data symbols x_1 and x_2

that BS sends to UN and UF.

In the context of NOMA, during the first $(1-\alpha)T/2$ block, considering the superposition of the BS transmit signal as in [24], the received signal at UN is formulated as

$$y_{UN} = h_A\left(\sqrt{\frac{(1-\beta)a_1P_S}{d_A^m}}x_1 + \sqrt{\frac{(1-\beta)a_2P_S}{d_A^m}}x_2\right) + n_0, \quad (4)$$

where n_0 denotes the additive white Gaussian noise (AWGN) at UN with zero mean and variance N_0. We additionally presume that $E\left[x_1^2\right] = E\left[x_2^2\right] = 1$.

From (4), we define the received signal-to-interference-plus-noise ratio (SINR) at UN for detecting x_2 at UF as

$$\gamma_{UN}^{x_2} = \frac{(1-\beta)\left|h_A\right|^2 d_A^{-m}a_2\rho}{(1-\beta)\left|h_A\right|^2 d_A^{-m}a_1\rho + 1}, \quad (5)$$

where $\rho = P_S/N_0$ stands for the transmit signal-to-noise ratio (SNR).

Having obtained the signals that BS sends, which are x_1 and x_2, UN decodes them using successive interference cancellation (SIC) [23], [28]. For UN to distinguish its own signal, x_1, we employ the received SNR described below

$$\gamma_{UN}^{x_1} = (1-\beta)\left|h_A\right|^2 d_A^{-m}a_1\rho. \quad (6)$$

B. From UN to UF: Information Transmission

UN consumes some harvested energy for its operation and the rest to DF the decoded signal x_2 to UF.

Thereby, during the second $(1-\alpha)T/2$ block, UF received the signal of

$$y_{UF} = \left(\sqrt{P_{UN}d_B^{-m}}x_2\right)h_B + n_0. \quad (7)$$

We substitute (3) into (7) to obtain the received SNR at UF as follows

$$\gamma_{UF}^{x_2} = \frac{\eta\rho[2\alpha + (1-\alpha)\beta]}{(1-\alpha)d_A^m d_B^m}\left|h_A\right|^2\left|h_B\right|^2. \quad (8)$$

C. Ergodic Outage Probability Performance

We analyse the system performance with a metric, namely, ergodic outage probability. It stands for the probability that the instantaneous capacity drops below the threshold C_{th} (bps/Hz).

Hence, for the NOMA JTAPS protocol, where UN can detect x_1 as described in (6), the instantaneous ergodic, $C_{UN}^{x_1}$ (bits/s/Hz) at UN, is obtainable from

$$C_{UN}^{x_1} = W\left(\frac{1-\alpha}{2}\right)\mathrm{E}\left[\log_2\left(1+\gamma_{UN}^{x_1}\right)\right], \quad (9)$$

where W is the bandwidth NOMA system.

Proposition 1.

In general, for X protocol at UN, the ergodic outage probability is expressed as

$$Po_{UN}^{x_1} = 1 - \mathcal{Q}\left(\left(\frac{10}{\ln(10)}\ln\left(c_1/c_2\right) - 2\mu_{h_A}\right)\Big/2\sigma_{h_A}\right), \quad (10)$$

where $c_1 = 2^{2\frac{C_{th}}{1-\alpha}} - 1$ *and* $c_2 = (1-\beta)d_1^{-m}a_1\rho$.

Proof.

Regarding to (7), we can calculate the cumulative distribution function (CDF) of the log-normally distributed RV $\left|h_A\right|^2$ as

$$Po_{UN}^{x_1} = Pr\left(\left|h_A\right|^2 < \frac{c_1}{(1-\beta)d_1^{-m}a_1\rho}\right) = F_{|h_A|^2}\left(\frac{c_1}{(1-\beta)d_1^{-m}a_1\rho}\right) = 1 - \mathcal{Q}\left(\left(\frac{10}{\ln(10)}\ln\left(\frac{c_1}{(1-\beta)d_1^{-m}a_1\rho}\right) - 2\mu_{h_A}\right)\Big/2\sigma_{h_A}\right), \quad (11)$$

where $Pr(.)$ is denoted as a probability function, and the Gaussian Q-function $\mathcal{Q}(x) = \int_x^\infty \frac{1}{\sqrt{2\pi}}\exp\left(-\frac{t^2}{2}\right)dt$.

The proof ends here.

To formulate the ergodic outage probability during $(1-\alpha)T/2$, the instantaneous ergodic capacity for the communication between BS and UN, UN and UF below must be utilized:

$$C_{UN}^{x_2} = W\left(\frac{1-\alpha}{2}\right)\mathrm{E}\left[\log_2\left(1+\gamma_{UN}^{x_2}\right)\right], \quad (12)$$

and

$$C_{UF}^{x_2} = W\left(\frac{1-\alpha}{2}\right)\mathrm{E}\left[\log_2\left(1+\gamma_{UF}^{x_2}\right)\right]. \quad (13)$$

Then we employ the received SNRs, $\gamma_{UN}^{x_2}$ in (5) and $\gamma_{UF}^{x_2}$ in (8), to express the ergodic outage probability at UF as follows

$$Po_{UF}^{x_2} = \Pr\left\{\min\left(C_{UN}^{x_2}, C_{UF}^{x_2}\right) < C_{th}\right\}. \quad (14)$$

Proposition 2.

The ergodic outage probability at UF is obtained from

$$Po_{UF}^{x_2} = 1 - \mathcal{Q}\left(\left(\frac{10}{\ln(10)}\ln\left(c_1/c_2\right) - 2\mu_{h_A}\right)\Big/2\sigma_{h_A}\right) + \frac{5}{\ln(10)\sqrt{2\pi\sigma_{h_A}^2}}\int_{x=c_1/c_2}^{\infty}\mathcal{I}_1(x)\times\mathcal{I}_2(x)dx, \quad (15)$$

where:

$$c_2 = d_1^{-m}(1-\beta)\left(a_2 - a_1c_1\right)\rho,$$

$$c_3 = \frac{\eta(2\alpha+\beta(1-\alpha))\rho}{(1-\alpha)d_A^m d_B^m},$$

$$\mathcal{I}_1(x) = \frac{1}{x}\exp\left(-\left(\frac{10}{\ln(10)}\ln(x) - 2\mu_{h_A}\right)^2 \Big/ 8\sigma_{h_A}^2\right),$$

and $\mathcal{I}_2(x) = 1-\mathcal{Q}\left(\left(\frac{10}{\ln(10)}\ln\left(c_1/c_3 x\right) - 2\mu_{h_B}\right)\Big/ 2\sigma_{h_B}\right).$

Proof.

The ergodic outage probability requires calculating two probabilities in (16) with the need of x_2 to be detected at both UN and UF as

$$\begin{aligned} Po_{UF}^{x_2} &= \Pr\left\{\min\left(C_{UN}^{x_2}, C_{UF}^{x_2}\right) < C_{th}\right\} = \\ &= 1-\Pr\left\{\min\left(C_{UN}^{x_2}, C_{UF}^{x_2}\right) \geq C_{th}\right\} = \\ &= 1-\Pr\left\{C_{UN}^{x_2} \geq C_{th}\right\} + \Pr\left\{C_{UN}^{x_2} \geq C_{th}, C_{UF}^{x_2} < C_{th}\right\}. \end{aligned} \quad (16)$$

We can calculate the first probability in (16) from

$$\begin{aligned} \Pr\left\{C_{UN}^{x_2} \geq C_{th}\right\} &= \Pr\left\{\frac{(1-\beta)|h_A|^2 d_A^{-m} a_2\rho}{(1-\beta)|h_A|^2 d_A^{-m} a_1\rho + 1} \geq c_1\right\} = \\ &= 1-\Pr\left\{|h_A|^2 < \frac{c_1}{d_1^{-m}(1-\beta)(a_2 - a_1 c_1)\rho}\right\} = \\ &= 1-F_{|h_A|^2}\left\{\frac{c_1}{d_1^{-m}(1-\beta)(a_2 - a_1 c_1)\rho}\right\} = \\ &= \mathcal{Q}\left(\left(\frac{10}{\ln(10)}\ln\left(c_1/c_2\right) - 2\mu_{h_A}\right)\Big/ 2\sigma_{h_A}\right). \end{aligned} \quad (17)$$

Regarding to two i.i.d. log-normal RVs $|h_A|^2$ and $|h_B|^2$, the second probability in (16) can be obtained from

$$\begin{aligned} &\Pr\left\{C_{UN}^{x_2}, C_{UF}^{x_2} < C_{th}\right\} = \\ &= \Pr\left(|h_A|^2 > \frac{c_1}{c_2}, |h_B|^2 < \frac{c_1}{c_3|h_A|^2}\right) = \\ &= \int_{c_1/c_2}^{\infty} f_{|h_A|^2}(x) F_{|h_B|^2}\left(c_1/c_3 x\right) \mathrm{d}x. \end{aligned} \quad (18)$$

Additionally, we have the CDF and PDF of the two RVs distributed log-normally as follows:

$$\begin{aligned} F_{|h_B|^2}\left(c_1/c_3 x\right) &= 1- \\ -\mathcal{Q}\left(\left(\frac{10}{\ln(10)}\ln\left(c_1/c_3 x\right) - 2\mu_{h_B}\right)\Big/ 2\sigma_{h_B}\right), \end{aligned} \quad (19)$$

and

$$f_{|h_A|^2}(x) = \frac{10}{x\ln(10)\sqrt{8\pi\sigma_{h_A}^2}} \times$$

$$\times \exp\left(-\left(\left(\frac{10}{\ln(10)}\ln(x) - 2\mu_{h_A}\right)^2\right)\Big/ 8\sigma_{h_A}^2\right). \quad (20)$$

Subsequently, we substitute (19) and (20) into (18), then combine the product with (17) to obtain the ergodic outage probability at UF, which is given in (15).

This is the end proof.

IV. RESULTS AND DISCUSSION

In this section, we study how the power splitting (PS) and time switching (TS) factors of the JTAPS protocol affect the system performance of NOMA over log-normal fading channels. In particular, we employ Monte Carlo simulations for the derived expressions with the following parameters in Table I.

Additionally, we assign the NOMA power allocation coefficients $a_1 = 0.2$ and $a_2 = 0.8$ for UN and UF. The SNR is $\rho = 20$ (dB). The theoretical and numerical results are plotted for comparison.

Figure 3 and Figure 4 illustrate the ergodic outage probability of UN and UF in EH NOMA scheme versus the varied EH PS factor and fixed TS factor. We investigate their relation in three different threshold cases.

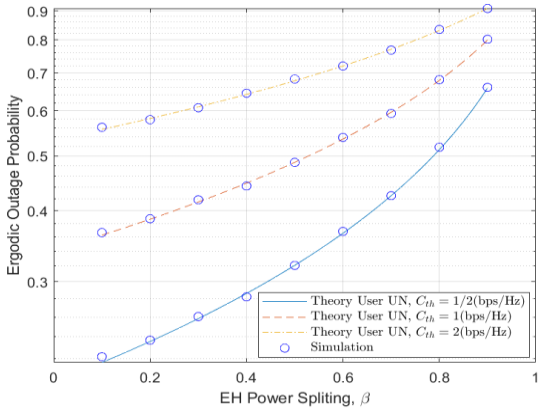

Fig. 3. Ergodic outage probability of UN in EH NOMA scheme versus the varied EH PS factor, β (EH TS fixed at $\alpha = 0.3$), with three different threshold values, C_{th}.

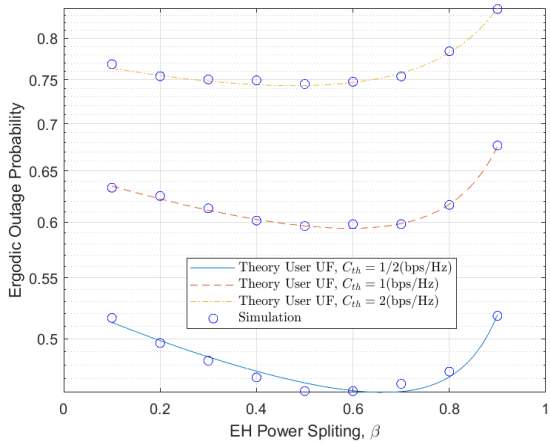

Fig. 4. Ergodic outage probability of UF in EH NOMA scheme versus the varied EH PS factor, β (EH TS fixed at $\alpha = 0.3$), with three different threshold values, C_{th}.

We can observe that for both graphs, the curve trends are similar. The lower the threshold C_{th}, the more significant the curve in comparison with the others is. Besides, at the lowest threshold value of $C_{th} = 1/2$ (bps/Hz), the system performs the best with a maximum ergodic outage probability of 0.66.

Specifically, in Fig. 3, the three curves gradually raise in association with the increase of the EH PS factor until they reach their maximum values at EH PS $\beta = 0.9$. As for Fig. 4, the three curves are slightly convex. They decrease at first to reach their minimum values at around $\beta = 0.6$, then quickly raise to their maximum values as well at EH PS $\beta = 0.9$ and the maximum ergodic outage probability of 0.52.

Besides, in Fig. 5 and Fig. 6, we plot the ergodic outage probability of UN and UF in EH NOMA scheme versus the varied EH TS factor and fixed PS factor. We analyse them as well in three different cases. Indeed, they are similar to the curves shown in Fig. 3 and Fig. 4, yet following remarkably more significant trends. In the same manner, the lower the C_{th}, the higher the system performance of both the UN and the UF is. Specifically, in Fig. 5, the ergodic outage probability is the highest at $\alpha = 0.6$, $\alpha = 0.8$, and $\alpha = 0.9$, respectively, for $C_{th} = 2$, $C_{th} = 1$, and $C_{th} = 1/2$. Additionally, in Fig. 6, the ergodic outage probability level is the lowest at $\alpha = 0.4$, $\alpha = 0.5$, and $\alpha = 0.6$, then drastically peak at $\alpha = 0.6$, $\alpha = 0.8$, and $\alpha = 0.9$, respectively, for $C_{th} = 2$, $C_{th} = 1$, and $C_{th} = 1/2$. Remarkably, similar to Fig. 3 and Fig. 4, the ergodic outage probability at the UN and UF are the best with $C_{th} = 1/2$.

TABLE I. PARAMETERS' SIMULATIONS.

Parameters	***Value***
W	5 (W)
η	80 %
m	2.7
$d_1 = d_2$	5 (m)
$\sigma_{h_1} = \sigma_{h_2}$	4 (dB)
$\mu_{h_1} = \mu_{h_2}$	3 (dB)

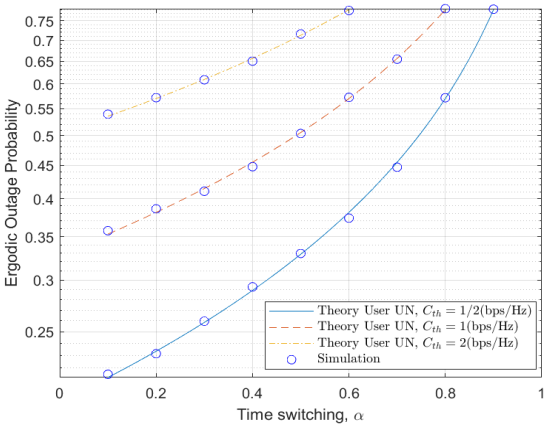

Fig. 5. Ergodic outage probability of UN in EH NOMA scheme versus the varied EH TS factor, α (EH PS factor fixed at $\beta = 0.3$), with three different threshold values, C_{th}.

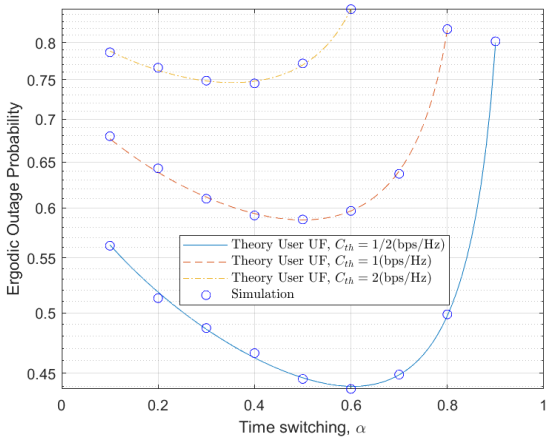

Fig. 6. Ergodic outage probability of UF in EH NOMA scheme versus the varied EH TS factor, α (EH PS factor fixed at $\beta = 0.3$), with three different threshold values, C_{th}.

V. CONCLUSIONS

To conclude, we investigate herein the ergodic outage probability of a hybrid protocol so-called "JTAPS" for NOMA-based EH wireless networks over indoor log-normal fading channels. Thanks to Monte Carlo simulations, we are able to assess the impact of different EH PS and EH TS factors on the system performance. Moreover, we can draw from the simulation results that the higher the capacity threshold value, the lower the system performance is. Generally speaking, the theoretical and numerical results correlate well with each other proving that the expressions that we derived can be employed for future studies.

CONFLICTS OF INTEREST

The authors declare that they have no conflicts of interest.

REFERENCES

[1] Y. Liu, Z. Qin, M. Elkashlan, Y. Gao, and L. Hanzo, "Enhancing the physical layer security of non-orthogonal multiple access in large-scale networks", *IEEE Transactions on Wireless Communications*, vol. 16, no. 3, pp. 1656–1672, 2017. DOI: 10.1109/TWC.2017.2650987.

[2] S. Timotheou and I. Krikidis, "Fairness for non-orthogonal multiple access in 5G systems", *IEEE Signal Processing Letters*, vol. 22, no. 10, pp. 1647–1651, 2015. DOI: 10.1109/LSP.2015.2417119.

[3] B. Di, L. Song, and Y. Li, "Sub-channel assignment, power allocation, and user scheduling for non-orthogonal multiple access networks", *IEEE Transactions on Wireless Communications*, vol. 15, no. 11, pp. 7686–7698, 2016. DOI: 10.1109/TWC.2016.2606100.

[4] M. A. S. Al-Adwany, "Efficient power allocation method for non orthogonal multiple access 5G systems", *International Journal of Electrical and Computer Engineering (IJECE)*, vol. 10, no. 2, pp. 2139–2150, 2020. DOI: 10.11591/ijece.v10i2.pp2139-2150.

[5] S. M. R. Islam, N. Avazov, O. A. Dobre, and K.-s. Kwak, "Power-domain non-orthogonal multiple access (NOMA) in 5G systems: Potentials and challenges", *IEEE Communications Surveys & Tutorials*, vol. 19, no. 2, pp. 721–742, 2017. DOI: 10.1109/COMST.2016.2621116.

[6] M. Hedayati and I.-M. Kim, "On the performance of NOMA in the two-user SWIPT system", *IEEE Transactions on Vehicular Technology*, vol. 67, no. 11, pp. 11258–11263, Nov. 2018. DOI: 10.1109/TVT.2018.2866612.

[7] H. T. Van *et al.*, "Outage performance analysis of non-orthogonal multiple access with time-switching energy harvesting", *Elektronika ir Elektrotechnika*, vol. 25, no. 3, pp. 85–91, 2019. DOI: 10.5755/j01.eie.25.3.23682.

[8] J. Tang *et al.*, "Optimization for maximizing sum secrecy rate in

SWIPT-enabled NOMA systems", *IEEE Access*, vol. 6, pp. 43440–43449, 2018. DOI: 10.1109/ACCESS.2018.2859935.

[9] J. Tang *et al*., "Energy efficiency optimization for NOMA with SWIPT", *IEEE Journal of Selected Topics in Signal Processing*, vol. 13, no. 3, pp. 452–466, 2019. DOI: 10.1109/JSTSP.2019.2898114.

[10] S. K. Zaidi, S. F. Hasan, and X. Gui, "Evaluating the ergodic rate in SWIPT-aided hybrid NOMA", *IEEE Communications Letters*, vol. 22, no. 9, pp. 1870–1873, 2018. DOI: 10.1109/LCOMM.2018.2849071.

[11] Q. Qi, X. Chen, and D. W. K. Ng, "Robust beamforming for NOMA-based cellular massive IoT with SWIPT", *IEEE Transactions on Signal Processing*, vol. 68, pp. 211–224, 2020. DOI: 10.1109/TSP.2019.2959246.

[12] H.-S. Nguyen, T.-S. Nguyen, V.-T. Vo, and M. Voznak, "Hybrid full-duplex/half-duplex relay selection scheme with optimal power under individual power constraints and energy harvesting", *Computer Communications*, vol. 124, pp. 31–44, 2018. DOI: 10.1016/j.comcom.2018.04.014.

[13] N. Zhao, F. Hu, Z. Li, and Y. Gao, "Simultaneous wireless information and power transfer strategies in relaying network with direct link to maximize throughput", *IEEE Transactions on Vehicular Technology*, vol. 67, no. 9, pp. 8514–8524, 2018. DOI: 10.1109/TVT.2018.2850747.

[14] F. K. Ojo and M. F. Mohd Salleh, "Throughput analysis of a hybridized power-time splitting based relaying protocol for wireless information and power transfer in cooperative networks", *IEEE Access*, vol. 6, pp. 24137–24147, 2018. DOI: 10.1109/ACCESS.2018.2828121.

[15] H.-S. Nguyen., D.-T. Do, and M. Voznak, "Two-way relaying networks in green communications for 5G: Optimal throughput and trade off between relay distance on power splitting-based and time switching-based relaying SWIPT", *AEU - International Journal of Electronics and Communications*, vol. 70, no. 12, pp. 1637–1644, 2016. DOI: 10.1016/j.aeue.2016.10.002.

[16] Y. Ye, Y. Li, L. Shi, R. Q. Hu, and H. Zhang, "Improved hybrid relaying protocol for DF relaying in the presence of a direct link", *IEEE Wireless Communications Letters*, vol. 8, no. 1, pp. 173–176, 2019. DOI: 10.1109/LWC.2018.2865476.

[17] D. Darsena, G. Gelli, and F. Verde, "Design and performance analysis of multiple-relay cooperative MIMO networks", *Journal of Communications and Networks*, vol. 21, no. 1, pp. 25–32, 2019. DOI: 10.1109/JCN.2019.000003.

[18] S. Sharma, A. S. Madhukumar, and R. Swaminathan, "Switching-based cooperative decode-and-forward relaying for hybrid FSO/RF networks", *IEEE/OSA Journal of Optical Communications and Networking*, vol. 11, no. 6, pp. 267–281, 2019. DOI: 10.1364/JOCN.11.000267.

[19] D. Wang, Y. Li, Y. Ye, H. Xia, and H. Zhang, "Joint time allocation and power splitting schemes for DF energy harvesting relaying networks", in *Proc. of 2017 IEEE 86th Vehicular Technology Conference (VTC-Fall)*, 2017, pp. 1–5. DOI: 10.1109/VTCFall.2017.8288115.

[20] L. T. T. Hoc *et al*., "Outage and bit error probability analysis in energy harvesting wireless cooperative networks", *Elektronika ir Elektrotechnika*, vol. 25, no. 5, pp. 69–74, 2019. DOI: 10.5755/j01.eie.25.5.24359.

[21] Z. Yang, Z. Ding, P. Fan, and N. Al-Dhahir, "The impact of power allocation on cooperative non-orthogonal multiple access networks with SWIPT", *IEEE Transactions on Wireless Communications*, vol. 16, no. 7, pp. 4332–4343, 2017. DOI: 10.1109/TWC.2017.2697380.

[22] Y. Xu *et al*., "Joint beamforming and power-splitting control in downlink cooperative SWIPT NOMA systems", *IEEE Transactions on Signal Processing*, vol. 65, no. 18, pp. 4874–4886, 2017. DOI: 10.1109/TSP.2017.2715008.

[23] Y. Alsaba, C. Y. Leow, and S. K. Abdul Rahim, "Full-duplex cooperative non-orthogonal multiple access with beamforming and energy harvesting", *IEEE Access*, vol. 6, pp. 19726–19738, 2018. DOI: 10.1109/ACCESS.2018.2823723.

[24] R. Hudec, S. Matuska, P. Kamencay, and M. Benco, "A smart IoT system for detecting the position of a lying person using a novel textile pressure sensor", *Sensors*, vol. 21, no. 1, p. 206, 2021. DOI: 10.3390/s21010206.

[25] S. Matuska, M. Paralic, and R. Hudec, "A smart system for sitting posture detection based on force sensors and mobile application", *Mobile Information Systems*, article ID 6625797, 2020. DOI: 10.1155/2020/6625797.

[26] M. Vestenicky, S. Matuska, R. Hudec, and P. Kamencay, "Sensor network proposal based on IoT for a prediction system of the power output from photovoltaic panels", in *Proc. of 2018 28th International Conference Radioelektronika (RADIOELEKTRONIKA)*, Prague, Czech Republic, 2018, pp. 1–4. DOI: 10.1109/RADIOELEK.2018.8376390.

[27] R. Hudec, S. Matuska, P. Kamencay, and L. Hudecova, "Concept of a wearable temperature sensor for intelligent textile", *Advances in Electrical and Electronic Engineering (AEEE)*, vol. 18, no. 2, pp. 92–98, 2020. DOI: 10.15598/aeee.v18i2.3610.

[28] H.-S. Nguyen, T. T. H. Ly, T.-S. Nguyen, V. V. Huynh, T.-L. Nguyen, and M. Voznak, "Outage performance analysis and SWIPT optimization in energy-harvesting wireless sensor network deploying NOMA", *Sensors*, vol. 19, no. 3, p. 613, 2019. DOI: 10.3390/s19030613.

[29] A. Laourine, A. Stephenne, and S. Affes, "On the capacity of log-normal fading channels", *IEEE Transactions on Communications*, vol. 57, no. 6, pp. 1603–1607, 2009. DOI: 10.1109/TCOMM.2009.06.070109.

[30] F. Mazzenga and R. Giuliano, "Log-normal approximation for VDSL performance evaluation", *IEEE Transactions on Communications*, vol. 64, no. 12, pp. 5266–5277, 2016. DOI: 10.1109/TCOMM.2016.2613108.

[31] M. Cheffena and M. Mohamed, "The application of lognormal mixture shadowing model for B2B channels", *IEEE Sensors Letters*, vol. 2, no. 3, pp. 1–4, 2018. DOI: 10.1109/LSENS.2018.2848296.

[32] K. M. Rabie, A. Salem, E. Alsusa, and M. Alouini, "Energy-harvesting in cooperative AF relaying networks over log-normal fading channels", in *Proc. of 2016 IEEE International Conference on Communications (ICC)*, Kuala Lumpur, 2016, pp. 1–7. DOI: 10.1109/ICC.2016.7511559.

[33] A. Salem, K. A. Hamdi, and E. Alsusa, "Physical layer security over correlated log-normal cooperative power line communication channels", *IEEE Access*, vol. 5, pp. 13909–13921, 2017. DOI: 10.1109/ACCESS.2017.2729784.

[34] K. M. Rabie, B. Adebisi, and M. Alouini, "Half-duplex and full-duplex AF and DF relaying with energy-harvesting in log-normal fading", *IEEE Transactions on Green Communications and Networking*, vol. 1, no. 4, pp. 468–480, 2017. DOI: 10.1109/TGCN.2017.2740258.

[35] Y. Liu, R. Xiao, J. Shen, H. Yang, and C. Yan, "Hybrid protocol for wireless energy harvesting network over log-normal fading channel", *The Journal of Engineering*, vol. 2018, no. 6, pp. 339–341, 2018. DOI: 10.1049/joe.2017.0892.